Journal of Applied and Natural Science
17(3), 1180 - 1192 (2025)
ISSN : 0974-9411 (Print), 2231-5209 (Online)
journals.ansfoundation.org

Research Article

Biosynthesis of silver nanoparticles using *Vitex negundo*: Pesticidal efficacy against *Spodoptera litura* and *Helicoverpa armigera* with a safety assessment

Yingying Jiang
Department of Life Sciences, CHRIST (Deemed to be University), Bangalore, India
Paari Kuppusamy Alagesan*
Department of Life Sciences, CHRIST (Deemed to be University), Bangalore, India

*Corresponding author. E-mail: paari.ka@christuniversity.in

Article Info
https://doi.org/10.31018/jans.v17i3.6708
Received: April 01, 2025
Revised: August 05, 2025
Accepted: August 17, 2025

How to Cite

Jiang, Y. and Alagesan, P. K. (2025). Biosynthesis of silver nanoparticles using *Vitex negundo*: Pesticidal efficacy against *Spodoptera litura* and *Helicoverpa armigera* with a safety assessment. *Journal of Applied and Natural Science*, 17(3), 1180 - 1192. https://doi.org/10.31018/jans.v17i3.6708

Abstract

Plant-based metallic nanoparticles hold promise for agricultural applications. This study investigated the biosynthesis of silver nanoparticles (AgNPs) using *Vitex negundo* leaf extract. It assessed their pesticidal properties and safety. AgNPs were synthesized via aqueous extract and characterized by UV–Vis spectroscopy, dynamic light scattering (DLS), Scanning electron microscopy (SEM), X-ray diffraction (XRD), and Fourier-transform infrared spectroscopy (FTIR) Characterization revealed a surface plasmon resonance (SPR) peak at 435 nm, an average particle size of 236.4 nm, and a stable zeta potential. SEM confirmed spherical morphology, XRD indicated a face-centred cubic (fcc) structure, and FTIR confirmed biomolecule-mediated capping and stabilization. Larvicidal bioassays showed that 5 mg/L AgNPs caused 78-89% mortality in *Spodoptera litura* and 83 -100% in *Helicoverpa armigera*. In both pests, oxidative stress was triggered. Catalase (CAT) activity increased by over 80% in *S.litura* and moderately in *H. armigera*. Glutathione-S-transferase (GST) activity declined post-treatment, from 9.4 to 5.0 mM/min/mg protein in *H. armigera* and from 1.0 to 0.7 mM/min/mg protein in *S. litura*, indicating impaired detoxification. In *Oreochromis urolepis*, AgNPs (5, 10, and 25 mg/L) induced oxidative stress without mortality. CAT activity decreased within 24 hours (72.4% at 5 mg/L) and remained suppressed by day 5 (36.7% at 25 mg/L). Superoxide dismutase (SOD) activity increased at 5 mg/L (19.8%) and 25 mg/L (54.8%), while GST initially declined but rebounded at higher concentrations. Reduced glutathione (GSH) levels increased by 24.3% at 25 mg/L, indicating adaptation. This study highlights that *V. negundo*-derived AgNPs are effective, eco-friendly biopesticides with minimal non-target toxicity.

Keywords: Silver nanoparticles, *Vitex negundo* leaves, Characterization, Larvicidal activity, Safety assessment

INTRODUCTION

In agriculture, silver nanoparticles (AgNPs) have gathered considerable interest due to their distinctive characteristics and potential benefits. Notably, AgNPs exhibit strong antimicrobial effectiveness against various species of fungi, bacteria, and viruses, effectively controlling plant pathogens and reducing crop diseases (Kumar *et al*., 2019; Neupane *et al*., 2022). In addition to their antimicrobial properties, AgNPs have shown potential as efficient insecticides and pesticides, thereby reducing reliance on chemical alternatives and mitigating associated environmental and health impacts (Qamar *et al*., 2021). However, their application as a sustainable, plant-based alternative to conventional pesticides remains underexplored. Most studies have focused on their role in antimicrobial protection and nano-fertilization (Soliman *et al*., 2020; Sabir *et al*., 2022).

Building on the promising applications of AgNPs, the use of plant-based methods for their synthesis has gained increasing trend in recent years. This approach not only aligns with eco-friendly and biocompatible practices but also proves to be cost-effective, making it a sustainable alternative to conventional synthesis methods (Zhang *et al*., 2021). Plant extracts, rich in biocompounds such as phenolics, amines, proteins, flavonoids, amide groups, alkaloids, terpenoids, and pigments, act as effective reducing and capping agents in the synthesis of AgNPs. (Sukweenadhi *et al*., 2021) demonstrated that ethanol extract of *Plantago major* L. leaves functioned as a stabilizing agent during a scale-

up synthesis trial, resulting in a ninefold increase in nanoparticle yield compared to small-scale synthesis. The observed monodisperse nature of these nanoparticles was attributed to the active binding of secondary metabolites to the nanoparticle surface.

Among the many plant sources studied for the green synthesis of AgNPs, *Vitex negundo* stands out due to its rich content of secondary metabolites, particularly terpenoids, which are highly valued in agriculture (Barreto *et al*., 2021). Native to China, India, and Indonesia, *V. negundo* has been traditionally used for various agricultural purposes (Ahuja *et al*., 2015), including promoting the growth of newly planted trees through fumigation and the application of organic mixtures, which may include its own leaves (Nalini, 2004). Its leaf extract, when combined with neem cake, has been shown to prevent flower shedding and premature pod fall in field beans (Sundaramari and Ranganathan, 2003), while the leaves themselves serve as green manure, enhancing soil fertility (Wang *et al*., 2022). Traditional pest control methods also leverage the insect-repellent properties of *V. negundo* leaves, further showcasing the plant's efficacy in controlling pests across various crops (Ahuja and Ahuja, 2008; Lal and Verma, 2006). These attributes not only highlight the plant's agricultural value but also underscore its promise as a sustainable origin for AgNPs synthesis. This study aimed to utilize *Vitex negundo* leaf extract in the biosynthesis of AgNPs and assess its potential as an eco-friendly pesticide by evaluating its characterization, efficacy, and safety.

MATERIALS AND METHODS

Green synthesis of AgNPs

Fresh, healthy *V. negundo* leaves were sourced from the Foundation for Revitalisation of Local Health Tradition (FRLHT), Bangalore, India. The plant species was verified and certified by the University of Transdisciplinary Health Sciences and Technology (TDU), Bangalore, India. Silver nitrate ($AgNO_3$, LR grade, Rankem) and other analytical-grade chemicals were obtained from local scientific suppliers in India.

Vitex negundo leaves were first shade-dried, followed by overnight drying in an oven at 50°C and then finely powdered. The leaf powder was combined with distilled water in a 1:10 ratio and subjected to Soxhlet extraction at 60°C for 24 hours. The obtained extracts were preserved at 5°C for subsequent synthesis. To optimize the green synthesis of AgNPs, the extract was blended with a silver nitrate solution at different concentrations (1 mM, 2 mM, 5 mM, and 10 mM) in varying ratios (1:1, 1:2, and 1:5). The mixtures were then shaken until a visible colour change occurred. The reactions were monitored using a UV-visible spectrophotometer across wavelengths from 400 to 500 nm, which corresponds to the characteristic surface plasmon resonance (SPR) band of AgNPs, indicative of free electron excitation(Ali *et al*., 2016). The mixture was subjected to centrifugation at 10,000 rpm for 20 minutes, and the resulting pellet was collected and oven-dried at 50°C overnight for further analysis.

Characterization of AgNPs

Nanoparticles are generally characterized in terms of their size, shape, dispersity, and surface area. The consistency of these properties is crucial for their performance in various applications. The synthesized AgNPs were analyzed using a range of analytical techniques. A UV-visible spectrophotometer (UV-1800, Shimadzu) was used to measure the maximum absorption in the range of 200-800 nm, with a resolution of 1 nm, enabling the detection of the reduction of Ag^+ ions to Ag^0 in the mixture (Valsalam *et al*., 2019). The average size and dispersity of AgNPs were assessed through Dynamic light scattering (DLS) and zeta potential measurements (ZEN 3600, Malvern Zetasizer)(Ravichandran *et al*., 2019). Structure and composition analysis were conducted using scanning electron microscopy (SEM, Apreo 2S, Thermo Fisher Scientific) in combination with energy-dispersive X-ray (EDX) analysis (Khan *et al*., 2021). The crystallinity of AgNPs was confirmed via X-ray diffraction (XRD) analysis, conducted at 5 VDC with Cu Kα radiation (λ = 1.54 Å), and a diffraction angle (2θ) ranging from 3° to 100° (Mohammed and Hawar, 2022). Functional groups and biomolecules were detected using Fourier-transform infrared spectroscopy (FTIR, QATR-S, SHIMADZU) over the range of 4000-500 cm^{-1}.

In vitro assessment of pesticide efficacy of G-AgNPs

The pesticidal activity of green-synthesized AgNPs was evaluated using *Spodoptera litura* and *Helicoverpa armigera* as target pests. A 5 mg/L G-AgNPs suspension was applied to the eggs and 1^{st} to 5^{th} instar larvae of both pests, with distilled water serving as a control. Hatchability and mortality rates were assessed 24 hours post-exposure. The impact of G-AgNPs on antioxidant enzyme activities was also analyzed to evaluate their physiological effects on the pest. 5^{th} instar larvae were homogenized with 0.1 M phosphate buffer (pH 7.4) for enzyme assays. The enzyme activities of CAT and GST were evaluated according to the protocols outlined below. For SOD assays, the reaction mixture was prepared by combining 2.85 mL of 0.05 M Tris -succinate buffer (pH 8.2) with 50 µL of the sample. The reaction was initiated upon adding 100 µL of 8 mM pyrogallol. Absorbance changes were measured at 412 nm every 30 seconds over a period of 3 minutes. For CAT assays, the reaction mixture was formed by combining 100 µL of sample with 2.8 mL of 0.1 M sodium phosphate buffer (pH 7.4). Upon adding 0.1 ml of H_2O_2, the mixture was measured at 240 nm for 3 min, with

absorbance readings taken every 30 seconds. The GST assay was conducted by combining 2.7 mL of 0.1 M sodium phosphate buffer (pH 7.4), 0.1 mL of 30 mM reduced glutathione, 100 µL of the sample, and 0.1 mL of 30 mM 1-chloro-2,4-dinitrobenzene (CDNB). Every 30 seconds for 3 minutes, absorbance at 340 nm was measured to monitor the reaction. The GR assay reaction mixture consisted of 500 µL of 0.2 M potassium phosphate buffer (pH 7.0), supplemented with 2 mM EDTA, 50 µL of 20 mM oxidised glutathione (GSSG), 50 µL of 2 mM NADPH (prepared in 10 mM Tris-HCl, pH 7.0), and 350 µL of deionized water. The reaction was triggered with 100 µL of the sample, and the enzymatic activity was assessed by monitoring the absorbance at 412 nm for 3 minutes.

Safety assessment of G-AgNPs in *Oreochromis urolepis*

The potential toxicity of green synthesized silver nanoparticles (AgNPs) was evaluated in *Oreochromis urolepis* (average weight: 0.97 ± 0.36 g), obtained from a local fish farm. Fish were maintained in 15 cm diameter fish bowls, each containing 1 L of tank water, at a controlled temperature of 25°C with aeration. The experimental setup involved exposing the fish to different concentrations of AgNPs (5 mg/L, 10 mg/L, and 25 mg/L) for 24 hours and 5 days, respectively, while the control group was kept under identical conditions without AgNPs exposure. The fish were monitored, and biochemical assays were conducted to assess oxidative stress and enzymatic activity. Antioxidant enzyme analysis was performed on the whole fish from both experimental and control groups. Fish tissues were homogenized in a 10% w/v solution of 0.1 M Tris HCl buffer (pH 7.4) and subjected to centrifugation at 6000 rpm, 4°C for 15 minutes to collect the supernatant. The supernatant was kept at -20°C and subsequently analyzed for later analysis of enzyme activity analysis. Superoxide dismutase (SOD), catalase (CAT), glutathione-S-transferase (GST) and reduced glutathione (GSH) levels were assessed to determine the oxidative stress response. All the measurements were conducted in triplicate.

To prepare the SOD reaction mixture, 120 µL of a 0.1 mM EDTA and 50 mM Na2CO3 solution, 80 µL of a 96 µM NBT solution, and 10 µL of a 0.6% Triton X-100 solution were added to each well of a microwell plate. After incubating for 10 minutes, 15 µL of hydroxylamine hydrochloride solution and 20 µL of the sample supernatant were added to the wells. The reaction proceeded for 3 minutes, and the absorbance was recorded at 560 nm to assess SOD activity (Kaur and Jindal, 2017). The CAT reaction was conducted in test tubes by combining 2.9 mL of 12.5 mM H_2O_2 and 0.067 M phosphate buffer (pH 7) with 0.1 mL of the sample supernatant. The reduction of absorbance measured at 240 nm was monitored every 30 seconds for 3 minutes to assess CAT activity(Sutha *et al*., 2020). The GST reaction mixture was prepared with 0.3 mL of the sample supernatant, 0.1 mL of 20 mM CDNB solution, and 2.5 mL of deionized water. After incubation at 37°C for 5 minutes, 0.1 mL of 20 mM GSH solution was introduced to initiate the reaction. The variation in absorbance at 340 nm was monitored at 30-second intervals for 5 minutes to determine GST activity(Ghosh *et al*., 2024). The GSH reaction solution was prepared by combining 0.01 mL of the sample supernatant with 0.2 mL of 0.2 M phosphate buffer. Following a 10-minute incubation, 0.1 mL of a 1 mM DTNB solution was added. The absorbance at 412 nm was then measured to determine the GSH level (Kaur and Jindal, 2017).

Statistical analysis

Triplicates were performed for all experiments, and the mean and standard error were calculated. To assess the significance differences, statistical analysis was conducted using one-way ANOVA, complemented by Tukey's post-hoc test, at a significance level of $p \leq 0.05$.

RESULT AND DISCUSSION

Characterization of AgNPs

UV-Visible analysis

One effective method for the swift characterization of metal nanoparticles is UV-visible spectroscopy (Wasilewska *et al*., 2023). The synthesis of AgNPs was verified through the measurement of surface plasmon resonance (SPR) in both the synthesis solution and *Vitex negundo* extract. The SPR absorption bands observed in metal nanoparticles result from the synchronized movement of free electrons, which resonate with the interacting light waves (Alharbi *et al*., 2022). The absorbance spectra between 400 to 500 nm are indicative of the formation of AgNPs in solution (Arif *et al*., 2022). As shown in Fig. 1, the combination prepared in a 1:2 volume ratio with 2mM $AgNO_3$ solution (S4) exhibited the most favourable spectral features, with a high-intensity peak observed at 435 nm after 24 h of incubation. The result is consistent with the previous study, which reported UV-absorption bands at 447 nm and 451 nm in plant-mediated green synthesis AgNPs (Nagesh *et al*., 2022). The observed peak shift is related to the particle size and degree of aggregation of the synthesized nanoparticles. As reported by Smitha *et al*. (2008), a sharp and narrow absorption peak suggests smaller nanoparticles, whereas a wider peak at an elevated wavelength indicates larger particle dimensions or aggregated AgNPs (Smitha *et al*., 2008).

Dynamic Light Scattering analysis

The size distribution of the green-synthesised AgNPs was characterized using DLS (Fig. 2). The analysis

indicated an average AgNPs size of approximately 236.4 nm and a polydispersity index (PDI) of 0.264. This indicates a homogeneous and broad size distribution (Sukweenadhi *et al*., 2021). This finding is completely compatible with previous studies, which reported similar size ranges and distributions (Nagesh *et al*., 2022; Ravichandran *et al*., 2019). The stability of the colloidal suspension was evaluated by assessing the zeta potential of the AgNPs. The result showed a distinct peak with an average zeta potential of -25.1 mV and a standard deviation of 5.53mV, suggesting moderate stability of the AgNPs suspension. Generally, zeta potential values around ±30 mV are considered indicative of a more stable colloidal system, resulting from electrostatic interactions, attraction, or repulsion among particles (Aryan *et al*., 2021). The measured zeta potential of -25.1mV in the current study suggested that AgNPs exhibited a degree of stability. The observed stability can be attributed to the reducing agents present in the *Vitex negundo* leaf extract, including phenolic and flavonoid compounds, which likely contribute to the negative charge on the AgNPs and enhance their electrostatic stability(Abdelbaky *et al*., 2022; Yassin *et al*., 2022).

Scanning Electron Microscopy analysis

Scanning Electron Microscopy (SEM) was employed to investigate the surface morphology of the green-synthesized AgNPs. At a magnification of 20,000x, the SEM image (Fig. 3A) revealed that most of AgNPs were spherical, although some particles exhibited signs of agglomeration. The particle diameter ranged from 10 to 88 nm. The predominance of spherical nanoparticles aligns with the typical morphology of AgNPs synthesized using plant extracts, where biomolecules in the extract serve as capping and stabilizing components, promoting the formation of spherical shapes (Nezhadian *et al*., 2021; Tamilarasi and Meena, 2020). The presence of agglomerated particles may be influenced by several factors, encompassing the concentration of the plant extract, the synthesis conditions, and interactions between the nanoparticles and biomolecules.

Energy Dispersive X-ray analysis

Energy dispersive X-ray analysis (EDX) was used to confirm the constituents of AgNPs. The results shown in Fig. 3B confirmed the presence of elemental silver, verifying the successful synthesis of AgNPs. The high silver content (77.21%) affirms that silver is the predominant element in the nanoparticles. The presence of oxygen (14.67%) and carbon (8.12%) confirms the role of organic compounds in the plant extract in reducing and stabilizing (Khatun *et al*., 2023). Similar results were observed for AgNPs synthesized from *Psophocarpus tetragonolobus* (L.) leaves, with a silver content of 70.38% and an oxygen content of 15.88% (Kamal Kumar *et al*., 2020).

X-ray Diffraction analysis

X-ray diffraction (XRD) analysis was applied to characterize the crystallographic structure of AgNPs. The XRD pattern (Fig. 4A) demonstrated distinct peaks at 2θ values of approximately 38.1°, 44.3°, 64.4°, 77.5°, and 81.5°. These peaks correspond to the (111), (200), (311), and (222) crystallographic planes of face-centred cubic (fcc) structure of silver (JCPDS card no. 04-0783), respectively, confirming the formation of pure AgNPs (Lanje *et al*., 2010; Yassin *et al*., 2022). The intensity and sharpness of the peaks suggest that the synthesized AgNPs exhibit high crystallinity (Ravichandran *et al*., 2019). This high crystallinity is crucial for the stability and functionality of AgNPs, indicating that the synthesis process was effective in producing well-formed and structurally consistent AgNPs. Additionally, the clear resolution of these peaks validates the effectiveness of the green synthesis method. It supports the purity of the NPs, which is essential for their potential application in various fields.

Fourier Transform Infrared Spectroscopy (FTIR) analysis

The FTIR analysis confirmed characteristic peaks indicative of various functional groups found in both the *Vitex negundo* extract and the green synthesized AgNPs (Fig. 4B). A broad O-H stretching vibration was observed at 3274.1 cm^{-1}, which signifies phenolic compounds, while the C-H asymmetric stretching vibrations at 2924.6 cm^{-1} associated with alkanes. Additionally, an N-H stretching band was detected at 1591.8 cm^{-1}, along with C-H stretching vibration at 788.9 cm^{-1}, suggesting the presence of alkanes and branched chain alkanes at 1394.3 cm^{-1}. Furthermore, the identification of oxidized nitrogen functional groups (N-O stretch) was recorded at 1309.0 cm^{-1}, along with an ether C-O stretch observed at 1038.8 cm^{-1} (Pawar and Kamble, 2017). In comparison to the extract, the synthesized AgNPs exhibited slight shifts and changes in peak intensity, indicating an interaction between the extracellular metabolites and silver ions. The reduction in intensity and shifts in peaks suggest successful capping and stabilization of AgNPs by the biomolecules from the extract, which is crucial for the nanoparticles' stability and bioactivity. Similar findings have been reported, confirming the role of biomolecules in the synthesis process (El-Ashmouny *et al*., 2022; Soliman *et al*., 2020).

***In vitro* and *in vivo* assessment of pesticide activity of G-AgNPs**

Hatchability and larvicidal activity

Table 1 denotes a significant reduction in hatchability for both *Spodoptera litura* (from 100% to 39%) and *Heli-*

coverpa armigera (from 100% to 22%) in the G-AgNPs treatment group compared to the control. AgNPs exhibited the most pronounced negative effects on hatchability, underscoring their potential as a toxic agent for pest management. Similarly, G-AgNPs demonstrated the highest larvicidal activity against both *S. litura* and *H. armigera*. Mortality rates (Table 2) ranged from 78-89% in *S. litura* (1st to 5th instars) and 83-100% in *H. armigera* (1st to 5th instars), showing particularly strong efficacy across all larval stages. These results align with the findings of Manimegalai *et al*. (2020), who reported larval mortality rates of 69.76% and 68.04% for *S. litura* and *H. armigera*, respectively, when treated with *Leonotis nepetifolia*–mediated AgNPs. Similarly, AgNPs synthesized from *Vernonia anthelmintica* seeds exhibited larvicidal activity with LC_{50} values of 56.42 µg/mL for *S. litura* and 63.65 µg/mL for *H. armigera* (Manimegalai *et al*., 2021). Further studies with AgNPs using *Dicrocephala integrifolia* leaf extract reported comparable results, with larval mortality rates of 69.76% for *S. litura* and 68.04% for *H. armigera,* respectively (Manimegalai *et al*., 2022). A previous study investigated the molecular interactions of key bioactive compounds from *Vitex negundo*, including oxalic acid, 6-ethyloct-3-yl hexyl ester, and (11Z)-13-methyl-11-tetradecenyl acetate, against critical target proteins in *S. litura* (Jiang and Paari, 2025). These proteins, namely acetylcholinesterase (AChE), carboxylesterase (CES), ecdysone receptor (EcR), and juvenile hormone-binding protein (JHBP), are essential regulators of neural transmission, detoxification, development, and reproduction, and are well-validated targets in insecticide research. Protein structures were prepared using standard protocols, including the removal of water molecules, correction of bond orders, addition of polar hydrogens, and automated protonation using the PyRx/AutoDock Vina workflow. Ligand-protein interactions with binding energies below −7.0 kcal/mol were considered to reflect strong binding affinity, indicating potential insecticidal relevance of these phytochemicals(Jiang and Paari, 2025). The high mortality rates observed could be attributed to the interaction between AgNPs and hormones that regulate protein synthesis and metabolic activity in insects (Baskar *et al*., 2014). These findings further support the potential of plant-based silver nanoparticles as effective agents for pest management.

The morphology effects on *Spodoptera litura* and *Helicoverpa armigera* larvae across their developmental instars revealed significant disruptions in larval physiology, indicating the strong larvicidal properties of G-AgNPs (Fig. 5 and 6). In the untreated control groups of both species, larvae exhibited normal growth patterns and maintained consistent pigmentation across the 1st to 5th instars. Conversely, larvae treated by G-AgNPs displayed progressive abnormalities, including dehydration, body deformation, and darkened pigmentation, reflecting severe physiological stress and tissue damage. In both *S. litura* and *H. armigera*, early instars showed marked dehydration and desiccation due to nanoparticle-induced cuticle damage and impaired water retention. Mid-instar insects exhibited wrinkled cuticles, reduced body mass, and growth deformities, likely resulting from oxidative stress and hormonal disruptions. Late instars developed darkened pigmentation, melanization, and black spots, indicative of cellular oxidative damage and apoptosis. Likewise, AgNPs synthesized using *Artemisia herba-alba* were shown to have significant effects on *Spodoptera littoralis* larvae, including dehydration, damage to the cuticle membrane, disintegration of the intestinal epithelium, and gonadal deformation (El-Ashmouny *et al*., 2022). The melanization abnormalities suggest that AgNPs could disrupt essential hormones and neuropeptides, such as juvenile hormone and ecdysone, both of which are crucial for insect growth and metamorphic regulation (Martínez-Cisterna *et al*., 2024). (Armstrong *et al*., 2013) observed that significantly reduced pigmentation in *D. melanogaster* exposed to AgNPs, with melanin levels being negligible or entirely absent. This reduction was attributed to oxidative stress caused by AgNPs, which disrupted copper transporters essential for copper absorption. This interference led to the inhibition of Cu-dependent enzymes, including copper/zinc superoxide dismutase (Cu/Zn SOD) and tyrosinase, both of which play pivotal roles in melanin synthesis. Consequently, this resulted in defects in pigmentation and irregularities in plant development (Ávalos *et al*., 2015). Overall, these findings highlight the significant physiological and morphological disruptions caused by G-AgNPs in agricultural pest species, demonstrating their potential utility as an effective tool for pest management.

Table 1. Ovicidal activity of G-AgNPs on *Spodoptera litura* and *Helicoverpa armigera*

Species	egg Hatchability (%)
S. litura	39.0 ± 0.1
H. armigera	22.0 ± 0.1

Biochemical assays

The biochemical and enzymatic responses of *Spodoptera litura* and *Helicoverpa armigera* larvae to green-synthesized silver nanoparticles (AgNPs) were analyzed, focusing on catalase (CAT) and glutathione-S-transferase (GST) activities (Fig. 7). Notable changes in CAT activity were observed in *S. litura*, with a substantial rise of over 380%, increasing from baseline levels to approximately 2,800 mM/min/mg protein after AgNP treatment. This sharp increase suggests enhanced neutralization of hydrogen peroxide to counteract oxidative stress, which is consistent with the finding of Yasur and Usha Rani (2015), who reported dose-related alterations in CAT, SOD, and POD, involved in

Table 2. larvicidal activity of G-AgNPs on *Spodoptera litura* and *Helicoverpa armigera*

mortality (%)	I instar	II instar	III instar	IV instar	V instar
Spodoptera. litura	78.00 ± 0.19	83.33 ± 0.17	72.33 ± 0.09	77.67 ± 0.09	88.67 ± 0.10
Helicoverpa armigera	100.00 ± 0.00	91.67 ± 0.14	83.33 ± 0.14	91.67 ± 0.14	100.00 ± 0.00

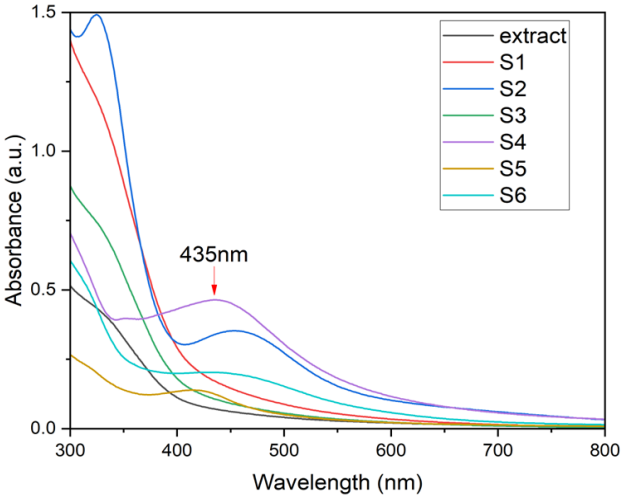

Fig. 1. *UV–vis spectra of Vitex negundo leaves extract and different green-synthesized groups of AgNPs. S1 - extract / $AgNO_3$(1mM) = 1:5; S2 - extract / $AgNO_3$(1mM) = 1:2; S3 - extract / $AgNO_3$(1mM) = 1:1; S4 - extract / $AgNO_3$ (2mM) = 1:2; S5 - extract / $AgNO_3$(5mM) = 1:2; S6 - extract / $AgNO_3$(10mM) = 1:2*

the removal of Reactive oxygen species (ROS). Highly responsive and cytotoxic molecules like ROS can disrupt lipids, proteins, and nucleic acids, leading to lipid peroxidation, protein denaturation, and mutations. The pronounced CAT activity in AgNP-treated *S. litura* larvae underscores their heightened oxidative stress and subsequent antioxidative response (Ibrahim *et al*., 2019). In contrast, *H. armigera* displayed a relatively modest increase in CAT activity, reaching around 1,000 mM/min/mg protein, suggesting a less pronounced antioxidant response compared to *S. litura.*

GST activity, a critical enzyme involved in detoxification, displayed contrasting patterns between the two species. In *H. armigera*, GST activity was significantly elevated in control larvae, reaching 9.4 mM/min/mg protein, while AgNP-treated larvae exhibited a decrease to 5.0 mM/min/mg protein, a reduction consistent with earlier reports suggesting that AgNPs may impair toxicity mitigation by interacting with GST enzymes (Parthiban *et al*., 2019). Conversely, in *S. litura*, GST activity remained relatively low, decreasing from 1.0 mM/min/mg protein in the control to 0.7 mM/min/mg protein in AgNP-treated larvae. The reduced GST activity in both species may result from the combined influence of pharmacologically active compounds on the AgNPs' surface, as noted by Jafir *et al*. (2021), which impairs the detoxification pathways and leads to metabolic disruption, growth inhibition, and mortality.

The observed biochemical responses align with the mechanisms by which AgNPs manifest their influence on insects, including physical disruption, genetic interference, and oxidative stress induction. AgNPs are known to reduce membrane permeability by crossing cellular barriers and interacting with genes that regulate membrane functions (Chen *et al*., 2019). Metal ions released from AgNPs in insects alter the enzyme activities related to detoxification mechanisms (Kafel *et al*., 2012), including antioxidant enzymes such as peroxidase (POD) and catalase (CAT), which play a role in removing harmful hydrogen peroxide (H_2O_2) and superoxide anions (Jomova *et al*., 2024). This disruption in enzymatic activity contributes to oxidative stress, which is linked to DNA damage. AgNPs penetrate the exoskeleton and interact with sulfur and phosphorus atoms

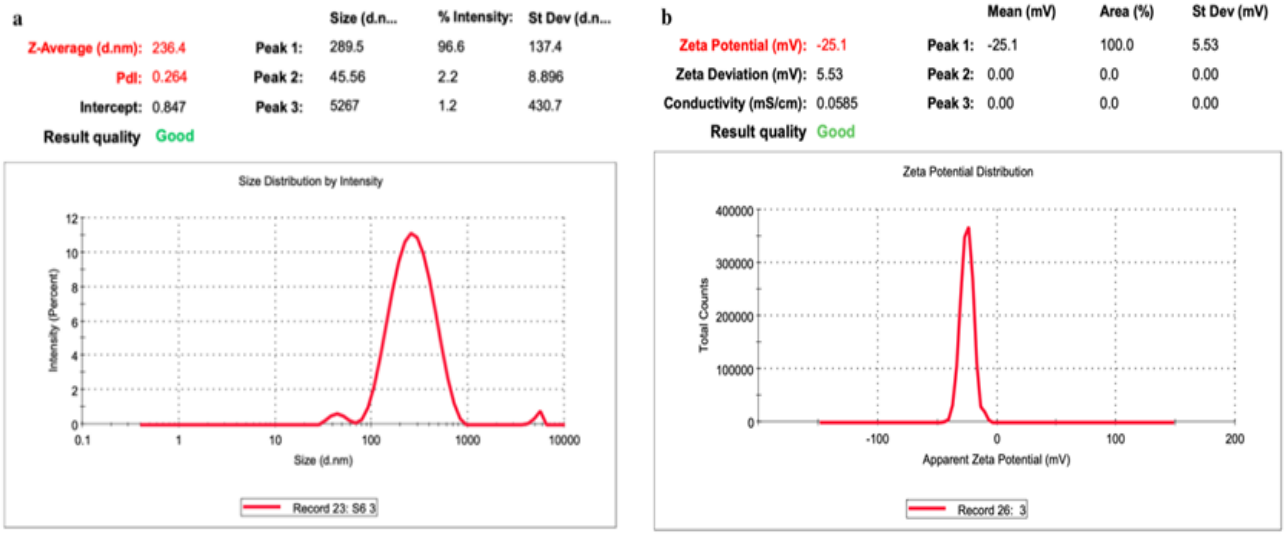

Fig. 2. *a DLS and b zeta potential pattern of green-synthesized AgNPs*

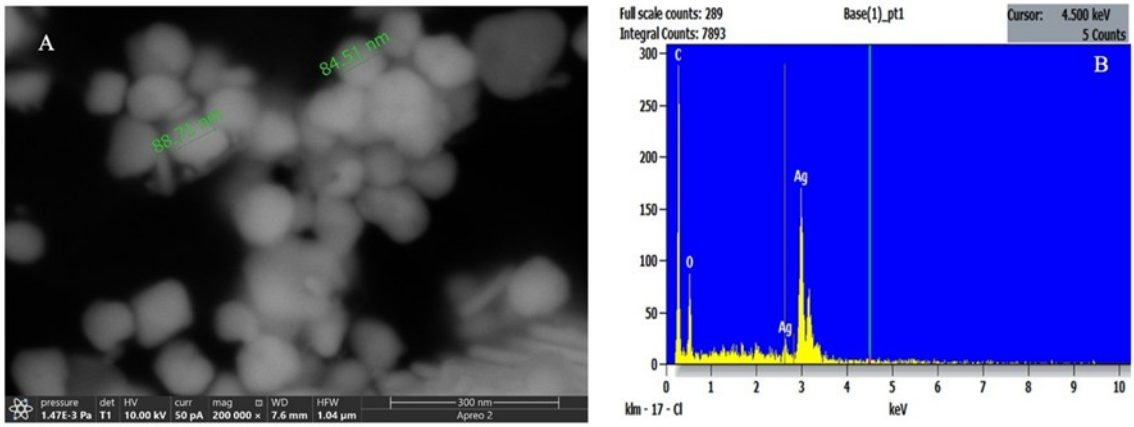

Fig. 3. *A: a SEM Image of green-synthesized AgNPs; B: a EDX image display elemental composition of biosynthesized AgNPs*

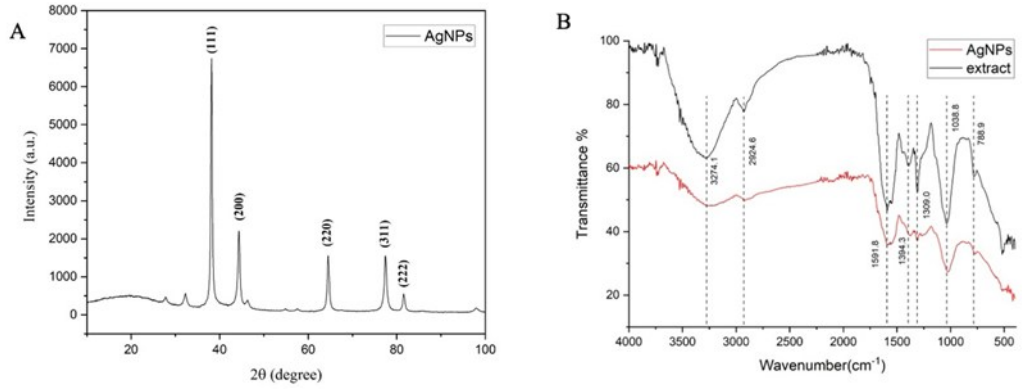

Fig. 4. *A: XRD pattern of green-synthesized AgNPs. B: FTIR spectra of Vitex negundo L. leaf extract and green-synthesized AgNPs*

in proteins, impairing transcription and translation, while disrupting DNA repair proteins such as p53 and Rad51 in insects like *Drosophila melanogaster* (Demir *et al*., 2011). Chronic toxicity is further evidenced by the expression of heat shock protein HSP70 and disruptions in dopamine and octopamine pathways, which impair development and fertility across generations (Posgai *et al*., 2009).

Safety assessment

The current study revealed the antioxidative enzyme responses to AgNPs exposure across different assays (Fig. 8). For SOD activity, no significant changes were observed in any treatment group 24 hours after AgNPs application, compared to the control. However, after 5 days of exposure, both lower (5 mg/L) and higher (25 mg/L) concentrations of AgNPs resulted in a notable increase in SOD activity (19.8% and 54.8%, respectively), while no significant change was observed at the intermediate concentration (10 mg/L). The absence of immediate changes in SOD activity suggests that the SOD defence system did not initially respond to AgNPs exposure, which contrasts with findings from other studies, where SOD activity often increases as an immediate adaptive response (Younas *et al*., 2022). The notable increase in SOD activity on the 5th day at both low and high concentrations suggests a delayed oxidative stress response, possibly due to the gradual accumulation of reactive oxygen species (ROS). The lack of significant change at the intermediate concentration may imply a dose-dependent threshold effect, where the antioxidant system's response is not linear or involves alternative antioxidant mechanisms that compensate for oxidative stress at this concentration. This dose-dependent response is consistent with findings from other studies, which suggest that the antioxidant defence system may only be triggered significantly beyond certain thresholds of ROS accumulation (Farag *et al*., 2023).

The efficiency of hydrogen peroxide (H_2O_2) decomposition by catalase (CAT) is directly proportional to its activity. After 24-hours of exposure, a significant decrease in CAT activity was observed across all AgNPs treatment groups, with the most pronounced reduction at the lower concentration (72.4%). On the 5th day, no substantial variations were observed at the 5 mg/L and 10 mg/L concentrations compared to the control; however, a significant reduction (36.7%) was noted at the higher concentration (25 mg/L). The substantial reduc-

Fig. 5. *Larvicidal effect of G-AgNPs on Spodoptera litura. A-E represent control larvae from 1st to 5th instar; F-J represent G-AgNPs treated larvae from 1st to 5th instar*

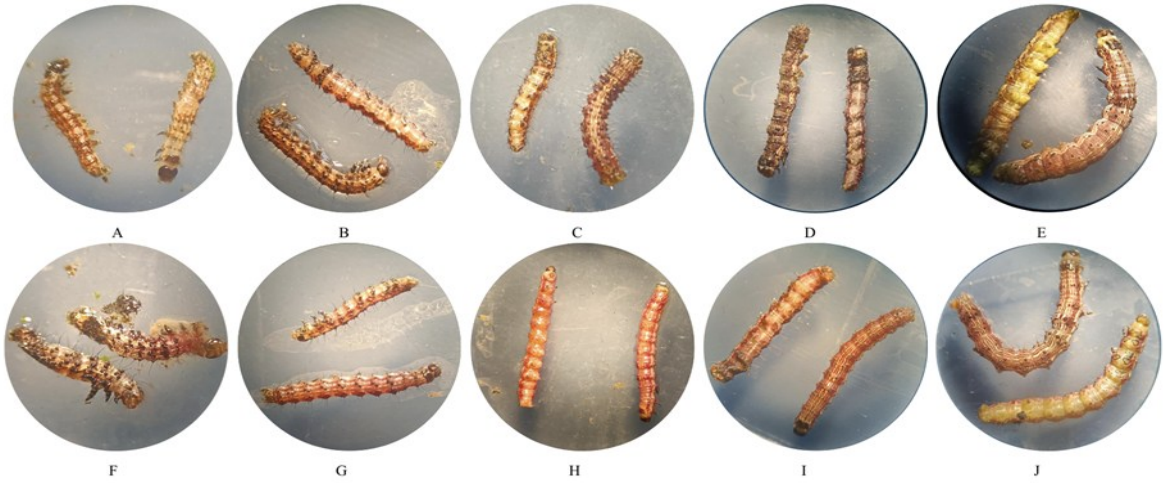

Fig. 6. *Larvicidal effect of G-AgNPs on Helicoverpa armigera. A-E represent control larvae from 1st to 5th instar; F-J represent G-AgNPs treated larvae from 1st to 5th instar*

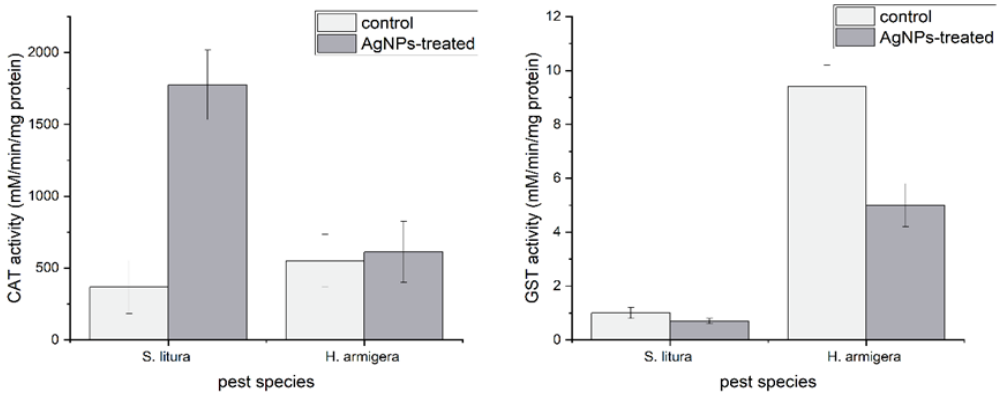

Fig. 7. *Oxidative stress biomarkers in Spodoptera litura and Helicoverpa armigera after exposure to AgNPs. Data is presented as Mean±S.D., n= 3*

tion in CAT activity after 24 hours suggests an immediate oxidative stress response in catalase (CAT) activity induced by AgNPs, which diminishes the enzyme's ability to decompose H_2O_2. This aligns with findings that metal nanoparticles can interfere with antioxidant enzyme activities due to their promotion of ROS production, which overwhelms the SOD-CAT system(Lee *et al*., 2012). The pronounced inhibition at the lower concentration indicates a high sensitivity of CAT activity to even minimal AgNP exposure, whereas the lack of

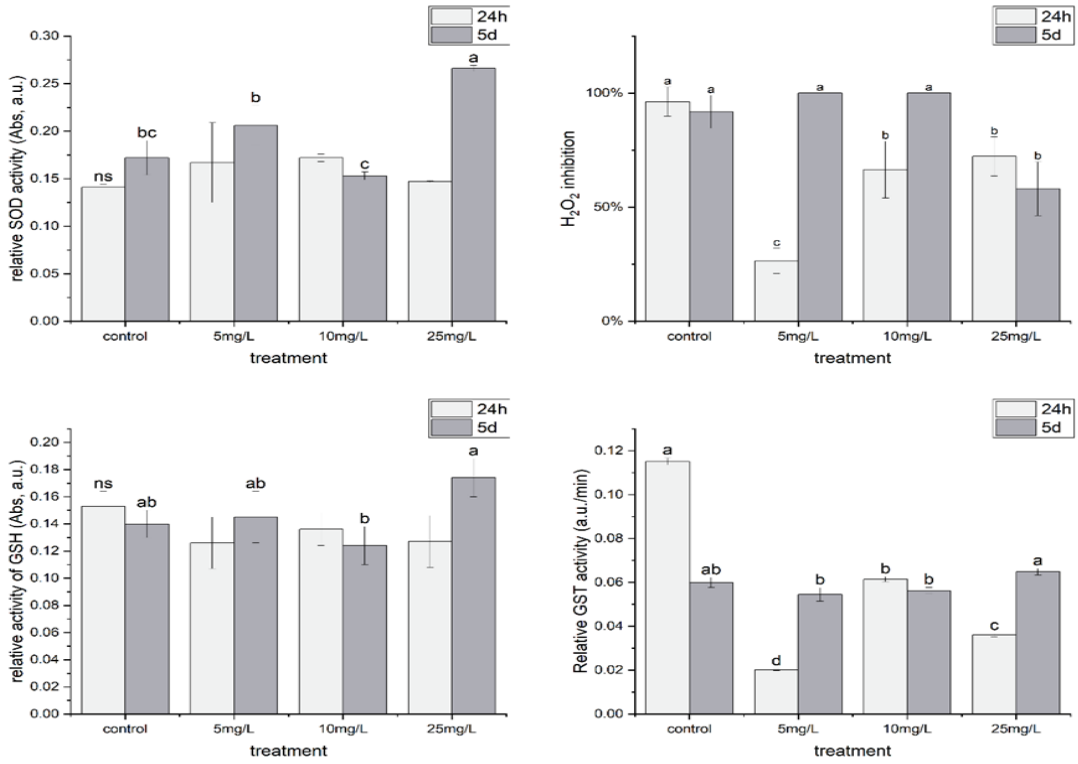

Fig. 8. *Antioxidant enzyme activity of Oreochromis urolepis on exposure to different concentrations of AgNPs. Data is presented as Mean±S.D., n= 3. Different lowercase letters show a significant difference at 0.05 level*

significant changes at 5 mg/L and 10 mg/L might reflect an adaptive or recovery mechanism. The persistent decrease at 25 mg/L suggests ongoing oxidative stress, consistent with other studies that show higher nanoparticle concentrations cause more severe oxidative stress (Ale *et al*., 2018; Lee *et al*., 2012). In contrast, lower AgNPs concentrations in some studies have been associated with increased antioxidant enzyme activities, likely due to differences in exposure duration, dose, and species sensitivity (Clark *et al*., 2019; Farkas *et al*., 2011).

The GSH level in *Oreochromis urolepis* exhibited fluctuations over the exposure duration. After 24 hours, no substantial differences were noted compared to the control at any treatment level. On the 5th day, GSH relative activity increased significantly by 24.3% at 25 mg/L, while no significant changes were observed at the lower and intermediate concentrations. The fluctuations in GSH levels indicate an adaptive antioxidant response to AgNP exposure. The lack of significant changes after 24 hours suggests that the initial exposure did not drastically alter GSH levels. The significant increase at 25 mg/L on the 5th day suggests an enhanced synthesis or accumulation of GSH as a defence mechanism against oxidative stress induced by AgNPs (Canli and Canli, 2020). This adaptive response at higher concentrations highlights the role of GSH in mitigating prolonged oxidative damage (Atli *et al*., 2016). Conversely, the absence of significant changes at lower and intermediate concentrations implies that these exposure levels did not elicit a substantial oxidative challenge or that the fish had sufficient baseline antioxidative capacity to cope with the stress.

The rate of absorbance increases at 340 nm revealing the GST activity in the organism. This study showed that after 24 hours of exposure, the control group exhibited the highest stress level. Various concentrations of AgNPs reduced stress levels. However, after 5-day exposure, higher AgNP concentrations demonstrated higher stress levels, while lower concentrations showed similar stress levels to the control. Mabrouk *et al*. (2021), found that exposing *Oreochromis niloticus* to chemical AgNPs at low concentrations (10 µg/L) enhanced the growth rates, feed efficiency, immunity, and antioxidant enzyme activities in Nile Tilapia (Mabrouk *et al*., 2021), However, higher concentrations led to detrimental effects, inducing toxicity in fish organs by diminishing antioxidant enzyme activity, disrupting the antioxidant system's ability to maintain safe ROS levels, inducing oxidative stress and potential cellular damage (Mansour *et al*., 2021). This highlights that green-synthesized AgNPs using *V. negundo* leaves might have an advantage by enhancing the safety profile of AgNPs, thereby reducing the application risks associated with their use.

Conclusion

The study successfully demonstrated the green synthesis of silver nanoparticles (AgNPs) using a *V. negundo*

leaves extract, confirming their formation and characterising their properties through various analytical techniques. The synthesized AgNPs exhibited spherical morphology, moderate stability, and good crystallinity, indicating their potential for agricultural applications. Furthermore, the pesticide effect of green-synthesized AgNPs was evident, showing notable larval toxicity against *S. litura* and *H. armigera*. The safety assessment of these plant-mediated AgNPs on *Oreochromis urolepis* highlighted a dose-dependent oxidative stress response, with lower concentrations posing minimal risks. These findings suggest that plant-mediated AgNPs offer not only an eco-friendly alternative to chemically synthesized nanoparticles but also a safer option for potential use in agriculture, thereby minimising environmental and health risks. Further studies will incorporate flexible docking approaches or molecular dynamics simulations, along with benchmark comparisons using known insecticides, to better account for receptor conformational variability and strengthen the validation of computational findings. Continued investigation is encouraged to thoroughly investigate the potential of plant-based nanoparticles in various agricultural settings.

ACKNOWLEDGEMENTS

The authors sincerely thank Christ (Deemed to be University) for providing the necessary facilities and resources to conduct this research.

Conflict of interest

The authors declare that they have no conflict of interest.

REFERENCES

1. Abdelbaky, A. S., Abd El-Mageed, T. A., Babalghith, A. O., Selim, S., & Mohamed, A. M. H. A. (2022). Green Synthesis and Characterization of ZnO Nanoparticles Using *Pelargonium odoratissimum* (L.) Aqueous Leaf Extract and Their Antioxidant, Antibacterial and Anti-inflammatory Activities. *Antioxidants*, *11*(8), Article 8. https://doi.org/10.3390/antiox11081444
2. Ahuja, S., Ahuja, S., & Ahuja, U. (2015). *Nirgundi* (*Vitex negundo*) – Nature's Gift to Mankind. *Asian Agri-History*, *19*(1), 5–32.
3. Ahuja, S., & Ahuja, U. (2008). Learning from farmers—Traditional rice production technology. *Asian Agri-History*, *12*(1), 19–41.
4. Ale, A., Rossi, A. S., Bacchetta, C., Gervasio, S., De La Torre, F. R., & Cazenave, J. (2018). Integrative assessment of silver nanoparticles toxicity in *Prochilodus lineatus* fish. *Ecological Indicators*, *93*, 1190–1198. https://doi.org/10/gt6n6h
5. Alharbi, N. S., Alsubhi, N. S., & Felimban, A. I. (2022). Green synthesis of silver nanoparticles using medicinal plants: Characterization and application. *Journal of Radiation Research and Applied Sciences*, *15*(3), 109–124. https://doi.org/10.1016/j.jrras.2022.06.012
6. Ali, M., Kim, B., Belfield, K. D., Norman, D., Brennan, M., & Ali, G. S. (2016). Green synthesis and characterization of silver nanoparticles using *Artemisia absinthium* aqueous extract—A comprehensive study. *Materials Science and Engineering: C*, *58*, 359–365. https://doi.org/10.1016/j.msec.2015.08.045
7. Arif, M., Ullah, R., Ahmad, M., Ali, A., Ullah, Z., Ali, M., Al-Joufi, F. A., Zahoor, M., & Sher, H. (2022). Green Synthesis of Silver Nanoparticles Using *Euphorbia wallichii* Leaf Extract: Its Antibacterial Action against Citrus Canker Causal Agent and Antioxidant Potential. *Molecules*, *27* (11), 3525. https://doi.org/10.3390/molecules27113525
8. Armstrong, N., Ramamoorthy, M., Lyon, D., Jones, K., & Duttaroy, A. (2013). Mechanism of silver nanoparticles action on insect pigmentation reveals intervention of copper homeostasis. *PLOS One*, *8*(1), e53186. https://doi.org/10.1371/journal.pone.0053186
9. Aryan, Ruby, & Mehata, M. S. (2021). Green synthesis of silver nanoparticles using Kalanchoe pinnata leaves (life plant) and their antibacterial and photocatalytic activities. *Chemical Physics Letters*, *778*, 138760. https://doi.org/10.1016/j.cplett.2021.138760
10. Atli, G., Canli, E. G., Eroglu, A., & Canli, M. (2016). Characterization of antioxidant system parameters in four freshwater fish species. *Ecotoxicology and Environmental Safety*, *126*, 30–37. https://doi.org/10/f799gv
11. Ávalos, A., Haza, A. I., Drosopoulou, E., Mavragani-Tsipidou, P., & Morales, P. (2015). *In vivo* genotoxicity assesment of silver nanoparticles of different sizes by the somatic mutation and recombination test (SMART) on *drosophila*. *Food and Chemical Toxicology*, *85*, 114–119. https://doi.org/10.1016/j.fct.2015.06.024
12. Barreto, I. C., de Almeida, A. S., & Sena Filho, J. G. (2021). Taxonomic Insights and Its Type Cyclization Correlation of Volatile Sesquiterpenes in *Vitex* Species and Potential Source Insecticidal Compounds: A Review. *Molecules*, *26*(21), Article 21. https://doi.org/10.3390/molecules26216405
13. Baskar, K., Muthu, C., & Ignacimuthu, S. (2014). Effect of pectolinaringenin, a flavonoid from *Clerodendrum phlomidis*, on total protein, glutathione S-transferase and esterase activities of *Earias vittella* and *Helicoverpa armigera*. *Phytoparasitica*, *42*(3), 323–331. https://doi.org/10.1007/s12600-013-0363-4
14. Canli, E. G., & Canli, M. (2020). Effects of aluminum, copper and titanium nanoparticles on the liver antioxidant enzymes of the Nile fish (*Oreochromis niloticus*). *Energy Reports*, *6*, 62–67. https://doi.org/10/gt6n2h
15. Chen, L., Meng, X., Gu, J., Fan, W., Abdlli, N., Peprah, F. A., Wang, N., Zhu, F., Lü, P., Ma, S., & Chen, K. (2019). Silver nanoparticle toxicity in silkworms: Omics technologies for a mechanistic understanding. *Ecotoxicology and Environmental Safety*, *172*, 388–395. https://doi.org/10.1016/j.ecoenv.2019.01.055
16. Clark, N. J., Boyle, D., Eynon, B. P., & Handy, R. D. (2019). Dietary exposure to silver nitrate compared to two forms of silver nanoparticles in rainbow trout: Bioaccumulation potential with minimal physiological effects. *Environmental Science: Nano*, *6*(5), 1393–1405. https://doi.org/10/gt6n6j

17. Demir, Eş., Vales, G., Kaya, B., Creus, A., & Marcos, R. (2011). Genotoxic analysis of silver nanoparticles in *drosophila*. *Nanotoxicology*, *5*(3), 417–424. https://doi.org/10.3109/17435390.2010.529176
18. El-Ashmouny, R. S., Rady, M. H., Merdan, B. A., El-Sheikh, T. A. A., Hassan, R. E., & El Gohary, E. G. E. (2022). Larvicidal and pathological effects of green synthesized silver nanoparticles from *Artemisia herba-alba* against *Spodoptera littoralis* through feeding and contact application. *Egyptian Journal of Basic and Applied Sciences*, *9*(1), 239–253. https://doi.org/10.1080/2314808X.2022.2063012
19. Farag, M. R., Abo-Al-Ela, H. G., Alagawany, M., Azzam, M. M., El-Saadony, M. T., Rea, S., Di Cerbo, A., & Nouh, D. S. (2023). Effect of Quercetin Nanoparticles on Hepatic and Intestinal Enzymes and Stress-Related Genes in Nile Tilapia Fish Exposed to Silver Nanoparticles. *Biomedicines*, *11*(3), Article 3. https://doi.org/10/gt5fgm
20. Farkas, J., Christian, P., Gallego-Urrea, J. A., Roos, N., Hassellöv, M., Tollefsen, K. E., & Thomas, K. V. (2011). Uptake and effects of manufactured silver nanoparticles in rainbow trout (*Oncorhynchus mykiss*) gill cells. *Aquatic Toxicology*, *101*(1), 117–125. https://doi.org/10/fd5b3w
21. Ghosh, D., Saha, S. K., Kaviraj, A., & Saha, S. (2024). Activity pattern of antioxidant enzymes in relation to the time of exposure of hexavalent chromium to nile tilapia *oreochromis niloticus*. *Ecotoxicology*. https://doi.org/10.1007/s10646-024-02832-1
22. Ibrahim, E., Fouad, H., Zhang, M., Zhang, Y., Qiu, W., Yan, C., Li, B., Mo, J., & Chen, J. (2019). Biosynthesis of silver nanoparticles using endophytic bacteria and their role in inhibition of rice pathogenic bacteria and plant growth promotion. *RSC Advances*, *9*(50), 29293–29299. https://doi.org/10.1039/C9RA04246F
23. Jiang, Y., & Paari, K. A. (2025). In silico screening of medicinal plant-derived compounds against *Spodoptera litura*. *Journal of Tropical Life Science*, *15*(1), 209–222. https://doi.org/10.11594/jtls.15.01.20
24. Jomova, K., Alomar, S. Y., Alwasel, S. H., Nepovimova, E., Kuca, K., & Valko, M. (2024). Several lines of antioxidant defense against oxidative stress: Antioxidant enzymes, nanomaterials with multiple enzyme-mimicking activities, and low-molecular-weight antioxidants. *Archives of Toxicology*, *98*(5), 1323–1367. https://doi.org/10.1007/s00204-024-03696-4
25. Kafel, A., Nowak, A., Bembenek, J., Szczygieł, J., Nakonieczny, M., & Świergosz-Kowalewska, R. (2012). The localisation of HSP70 and oxidative stress indices in heads of *spodoptera exigua* larvae in a cadmium-exposed population. *Ecotoxicology and Environmental Safety*, *78*, 22–27. https://doi.org/10.1016/j.ecoenv.2011.10.024
26. Kamal Kumar, V., Muthukrishnan, S., & Rajalakshmi, R. (2020). Phytostimulatory effect of phytochemical fabricated nanosilver (AgNPs) on *Psophocarpus tetragonolobus* (L.) DC. seed germination: An insight from antioxidative enzyme activities and genetic similarity studies. *Current Plant Biology*, *23*, 100158. https://doi.org/10.1016/j.cpb.2020.100158
27. Kaur, M., & Jindal, R. (2017). Oxidative Stress Response in Liver, Kidney and Gills of Ctenopharyngodon Idellus (Cuvier & Valenciennes) Exposed To Chlorpyrifos. *MOJ Biology and Medicine*, *1*, 00021. https://doi.org/10.15406/mojbm.2017.01.00021
28. Khan, A. K., Renouard, S., Drouet, S., Blondeau, J.-P., Anjum, I., Hano, C., Abbasi, B. H., & Anjum, S. (2021). Effect of UV irradiation (A and C) on *casuarina equisetifolia*-mediated biosynthesis and characterization of antimicrobial and anticancer activity of biocompatible zinc oxide nanoparticles. *Pharmaceutics*, *13*(11), 1977. https://doi.org/10.3390/pharmaceutics13111977
29. Khatun, M., Khatun, Z., Karim, Md. R., Habib, Md. R., Rahman, Md. H., & Aziz, Md. A. (2023). Green synthesis of silver nanoparticles using extracts of *Mikania cordata* leaves and evaluation of their antioxidant, antimicrobial and cytotoxic properties. *Food Chemistry Advances*, *3*, 100386. https://doi.org/10/gt6nvg
30. Kumar, A., Rakshit, R., Bhowmik, A., Mandal, N., Das, A., & Adhikary, S. (2019). Nanoparticle-Induced Changes in Resistance and Resilience of Sensitive Microbial Indicators towards Heat Stress in Soil. *Sustainability*, *11*(3), Article 3. https://doi.org/10.3390/su11030862
31. Lal, C., & Verma, L. R. (2006). Use of certain bio-products for insect-pest control. *Indian Journal of Traditional Knowledge*, *5*(1), 79–82.
32. Lanje, A., Sharma, S., & Pode, R. (2010). Synthesis of silver nanoparticles: A safer alternative to conventional antimicrobial and antibacterial agents. *Journal of Chemical and Pharmaceutical Research*, *2*, 478–483.
33. Lee, B., Duong, C. N., Cho, J., Lee, J., Kim, K., Seo, Y., Kim, P., Choi, K., & Yoon, J. (2012). Toxicity of Citrate-Capped Silver Nanoparticles in Common Carp (*Cyprinus carpio*). *Journal of Biomedicine and Biotechnology*, *2012* (1), 1–14. https://doi.org/10/gcff8h
34. Mabrouk, M. M., Mansour, A. T., Abdelhamid, A. F., Abualnaja, K. M., Mamoon, A., Gado, W. S., Matter, A. F., & Ayoub, H. F. (2021). Impact of aqueous exposure to silver nanoparticles on growth performance, redox status, non-specific immunity, and histopathological changes of Nile Tilapia, *Oreochromis niloticus*, challenged with *Aeromonas hydrophila*. *Aquaculture Reports*, *21*, 100816. https://doi.org/10/gt5fhh
35. Manimegalai, T., Raguvaran, K., Kalpana, M., Ajarem, A. J. S., Allam, A. A., Khim, J. S., & Maheswaran, R. (2022). Bio efficacy of synthesised silver nanoparticles using *dicrocephala integrifolia* leaf extract and their insecticidal activity. *Materials Letters*, *314*, 131860. https://doi.org/10.1016/j.matlet.2022.131860
36. Manimegalai, T., Raguvaran, K., Kalpana, M., & Maheswaran, R. (2021). Facile Synthesis of Silver Nanoparticles Using *Vernonia anthelmintica* (L.) Willd. And Their Toxicity Against *Spodoptera litura* (Fab.), *Helicoverpa armigera* (Hüb.), i Linn. And *Culex quinquefasciatus* Say. *Journal of Cluster Science*. https://doi.org/10.1007/s10876-021-02151-z
37. Mansour, W. A. A., Abdelsalam, N. R., Tanekhy, M., Khaled, A. A., & Mansour, A. T. (2021). Toxicity, inflammatory and antioxidant genes expression, and physiological changes of green synthesis silver nanoparticles on Nile tilapia (*Oreochromis niloticus*) fingerlings. *Comparative Biochemistry and Physiology Part C: Toxicology & Pharmacology*, *247*, 109068. https://doi.org/10.1016/j.cbpc.2021.109068
38. Martínez-Cisterna, D., Rubilar, O., Tortella, G., Chen, L., Chacón-Fuentes, M., Lizama, M., Parra, P., & Bardehle,

L. (2024). Silver nanoparticles as a potent nanopesticide: Toxic effects and action mechanisms on pest insects of agricultural importance—a review. *Molecules*, *29*(23), Article 23. https://doi.org/10.3390/molecules29235520

39. Mohammed, G. M., & Hawar, S. N. (2022). Green Biosynthesis of Silver Nanoparticles from *Moringa oleifera* Leaves and Its Antimicrobial and Cytotoxicity Activities. *International Journal of Biomaterials*, *2022*(1), 1–10. https://doi.org/10/gt6n5f
40. Nagesh, M. R., Kumar, N., Khan, J. M., Ahmed, M. Z., Kavitha, R., Kim, S.-J., & Vijayakumar, N. (2022). Green synthesis and pharmacological applications of silver nanoparticles using ethanolic extract of *Salacia chinensis* L. *Journal of King Saud University - Science*, *34*(7), 102284. https://doi.org/10.1016/j.jksus.2022.102284
41. Nalini, S. (2004). Vishvavallabha (Dear to the World. The science of plant life). *Agri-History Bulletin*, *5*, 134.
42. Neupane, N. P., Kushwaha, A. K., Karn, A. K., Khalilullah, H., Uzzaman Khan, M. M., Kaushik, A., & Verma, A. (2022). Anti-bacterial efficacy of bio-fabricated silver nanoparticles of aerial part of *Moringa oleifera lam*: Rapid green synthesis, *In-Vitro* and *In-Silico* screening. *Biocatalysis and Agricultural Biotechnology*, *39*, 102229. https://doi.org/10.1016/j.bcab.2021.102229
43. Nezhadian, T. A., Majidian, P., Gerami, M., & Ramezani, M. (2021). EFFECT OF GREEN SYNTHESIZED SILVER NANOPARTICLES ON CARNOSIC ACID CONTENT AND PHYSIO-BIOCHEMICAL PROPERTIES OF *Rosmarinus Officinalis* L. *Journal of the Chilean Chemical Society*, *66*(3), 5251–5258. https://doi.org/10.4067/S0717-97072021000305251
44. Parthiban, E., Ramachandran, M., Jayakumar, M., & Ramanibai, R. (2019). Biocompatible green synthesized silver nanoparticles impact on insecticides resistant developing enzymes of dengue transmitted mosquito vector. *SN Applied Sciences*, *1*(10), 1282. https://doi.org/10.1007/s42452-019-1311-9
45. Pawar, S., & Kamble, V. (2017). Phytochemical screening, elemental and functional group analysis of *Vitex negundo* L. leaves. *International Journal of Pharmacy and Pharmaceutical Sciences*, *9*(6), 226. https://doi.org/10.22159/ijpps.2017v9i6.18093
46. Posgai, R., Ahamed, M., Hussain, S. M., Rowe, J. J., & Nielsen, M. G. (2009). Inhalation method for delivery of nanoparticles to the drosophila respiratory system for toxicity testing. *Science of the Total Environment*, *408*(2), 439–443. https://doi.org/10.1016/j.scitotenv.2009.10.008
47. Qamar, S. U. R., Tanwir, S., Khan, W. A., Altaf, J., & Ahmad, J. N. (2021). Biosynthesis of silver nanoparticles using *Ocimum tenuiflorum* extract and its efficacy assessment against *Helicoverpa armigera*. *International Journal of Pest Management*, *70*(3), 375–383. https://doi.org/10.1080/09670874.2021.1980244
48. Ravichandran, V., Vasanthi, S., Shalini, S., Shah, S. A. A., Tripathy, M., & Paliwal, N. (2019). Green synthesis, characterization, antibacterial, antioxidant and photocatalytic activity of *Parkia speciosa* leaves extract mediated silver nanoparticles. *Results in Physics*, *15*, 102565. https://doi.org/10.1016/j.rinp.2019.102565
49. Sabir, S., Arshad, M., Ilyas, N., Naz, F., Amjad, M. S., Malik, N. Z., & Chaudhari, S. K. (2022). Protective role of foliar application of green-synthesized silver nanoparticles against wheat stripe rust disease caused by *Puccinia striiformis*. *Green Processing and Synthesis*, *11*(1), 29–43. https://doi.org/10.1515/gps-2022-0004
50. Smitha, S. L., Nissamudeen, K. M., Philip, D., & Gopchandran, K. G. (2008). Studies on surface plasmon resonance and photoluminescence of silver nanoparticles. *Spectrochimica Acta Part A: Molecular and Biomolecular Spectroscopy*, *71*(1), 186–190. https://doi.org/10/c6gh22
51. Soliman, M., Qari, S. H., Abu-Elsaoud, A., El-Esawi, M., Alhaithloul, H., & Elkelish, A. (2020). Rapid green synthesis of silver nanoparticles from blue gum augment growth and performance of maize, fenugreek, and onion by modulating plants cellular antioxidant machinery and genes expression. *Acta Physiologiae Plantarum*, *42*(9), 148. https://doi.org/10.1007/s11738-020-03131-y
52. Sukweenadhi, J., Setiawan, K. I., Avanti, C., Kartini, K., Rupa, E. J., & Yang, D.-C. (2021). Scale-up of green synthesis and characterization of silver nanoparticles using ethanol extract of *Plantago major* L. leaf and its antibacterial potential. *South African Journal of Chemical Engineering*, *38*(1), 1–8. https://doi.org/10.1016/j.sajce.2021.06.008
53. Sundaramari, M., & Ranganathan, T. T. (2003). *Indigenous agricultural practices for sustainable farming*. Agrobios (India). https://books.google.co.in/books?id=7j2KAAAACAAJ
54. Sutha, J., Anila, P. A., Umamaheswari, S., Ramesh, M., Narayanasamy, A., Poopal, R.-K., & Ren, Z. (2020). Biochemical responses of a freshwater fish *cirrhinus mrigala* exposed to tris(2-chloroethyl) phosphate (TCEP). *Environmental Science and Pollution Research*, *27*(27), 34369–34387. https://doi.org/10.1007/s11356-020-09527-0
55. Tamilarasi, P., & Meena, P. (2020). Green synthesis of silver nanoparticles (Ag NPs) using Gomphrena globosa (Globe amaranth) leaf extract and their characterization. *Materials Today: Proceedings*, *33*, 2209–2216. https://doi.org/10.1016/j.matpr.2020.04.025
56. Valsalam, S., Agastian, P., Arasu, M. V., Al-Dhabi, N. A., Ghilan, A.-K. M., Kaviyarasu, K., Ravindran, B., Chang, S. W., & Arokiyaraj, S. (2019). Rapid biosynthesis and characterization of silver nanoparticles from the leaf extract of *Tropaeolum majus* L. and its enhanced *in-vitro* antibacterial, antifungal, antioxidant and anticancer properties. *Journal of Photochemistry and Photobiology B: Biology*, *191*, 65–74. https://doi.org/10.1016/j.jphotobiol.2018.12.010
57. Wang, F., Cui, H., He, F., Liu, Q., Zhu, Q., Wang, W., Liao, H., Yao, D., Cao, W., & Lu, P. (2022). The green manure (*astragalus sinicus* L.) improved rice yield and quality and changed soil microbial communities of rice in the karst mountains area. *Agronomy*, *12*(8), Article 8. https://doi.org/10.3390/agronomy12081851
58. Wasilewska, A., Klekotka, U., Zambrzycka, M., Zambrowski, G., Święcicka, I., & Kalska-Szostko, B. (2023). Physico-chemical properties and antimicrobial activity of silver nanoparticles fabricated by green synthesis. *Food Chemistry*, *400*, 133960. https://doi.org/10.1016/j.foodchem.2022.133960
59. Yassin, M. T., Mostafa, A. A.-F., Al-Askar, A. A., & Al-Otibi, F. O. (2022). Facile Green Synthesis of Silver Nanoparticles Using Aqueous Leaf Extract of *Origanum majorana* with Potential Bioactivity against Multidrug Resistant Bacterial Strains. *Crystals*, *12*(5), Article 5. https://doi.org/10.3390/cryst12050603

60. Younas, W., Khan, F. U., Zaman, M., Lin, D., Zuberi, A., & Wang, Y. (2022). Toxicity of synthesized silver nanoparticles in a widespread fish: A comparison between green and chemical. *Science of The Total Environment*, *845*, 157366. https://doi.org/10.1016/j.scitotenv.2022.157366

61. Zhang, H., Chen, S., Jia, X., Huang, Y., Ji, R., & Zhao, L. (2021). Comparation of the phytotoxicity between chemically and green synthesized silver nanoparticles. *Science of The Total Environment*, *752*, 142264. https://doi.org/10.1016/j.scitotenv.2020.142264